

$$\begin{aligned}
N_2 &= \pi^{-3/4} [(2a)^{-3} + 2z(a^2 + b^2)^{-3/2} + z^2(2b)^{-3}]^{-1/2} \pi^{3/2}, \\
N_3 &= \left( \frac{\beta^2}{\sqrt{3}\pi} \right)^{3/2}, \quad N_4 = \left( \frac{\alpha^3}{2\pi^{3/2}} \right)^{3/2}, \quad N_6 = \left( \frac{\gamma^5}{\sqrt{6}\pi^{5/2}} \right)^{3/2}, \\
N_{10} &= \left( \frac{27}{\pi q_0^3} \right)^{1/2} (2\pi)^3, \quad Q_3 = \left( \frac{4\pi}{\beta^2} \right)^{3/2} N_3, \\
F_2 &= \left( \frac{3\pi}{\beta^2} \right)^{3/2}, \quad F_3 = \left( \frac{8\pi}{3\alpha^2} \right)^{3/2}, \\
F_4 &= \pi^{-3/4} [(2c)^{-3} + 2y(c^2 + d^2)^{-3/2} + y^2(2d)^{-3}]^{-1/2} \pi^{3/2}, \\
G_4 &= \left( \frac{3\pi}{2\gamma^2} \right)^{3/2}, \quad G_3 = \left( \frac{8\pi}{3\gamma^2} \right)^{3/2}; \\
a &= 60 \text{ MeV}, \quad a_0 = 0.84 \times 10^{-13} \text{ m}, \quad \alpha = 146 \text{ MeV}, \\
b &= 128 \text{ MeV}, \quad z = 1.03, \quad \beta = 155 \text{ MeV}, \\
c &= 56 \text{ MeV}, \quad y = -2.42, \quad \gamma = 128 \text{ MeV}, \\
d &= 156 \text{ MeV}.
\end{aligned}$$

Furthermore, we use

$$\lambda = 1.18, \quad G_m p^2 = 1.02 \times 10^{-5}.$$

<sup>†</sup>For a discussion of the impulse model, see G. F. Chew and G. C. Wick, *Phys. Rev.* **85**, 636 (1952); M. Gell-Mann and M. L. Goldberger, *Phys. Rev.* **91**, 398 (1953); G. F. Chew and M. L. Goldberger, *Phys. Rev.* **87**, 788 (1952); see also Ref. 5.

<sup>‡</sup>The fields  $\psi(x)$  are expanded in plane waves via

$$\begin{aligned}
\psi(x) &= (2\pi)^{-3/2} \int d^3k \left( \frac{m}{\epsilon} \right)^{1/2} \sum_{r=1,2} a^{(r)}(k) u^{(r)}(k) e^{ik \cdot x} \\
&\quad + b^{(r)}(k) v^{(r)}(k) e^{ik \cdot x},
\end{aligned}$$

where  $r$  refers to the spin indices,  $u(k)$  and  $v(k)$  are Dirac spinors for particle and antiparticle, and the creation and annihilation operators  $a^\dagger, b^\dagger$  and  $a, b$  satisfy the anticommutation relations

$$\begin{aligned}
\{a^{(r)}(k), a^{(s)}(q)\} &= \delta_{rs} \delta^3(k - q), \\
\{b^{(r)}(k), b^{(s)\dagger}(q)\} &= \delta_{rs} \delta^3(k - q), \\
\{b^{(r)}(k), a^{(s)}(q)\} &= \{b^{(r)\dagger}(k), a^{(s)}(q)\} = 0, \\
\{b^{(r)}(k), a^{(s)}(q)\} &= \{b^{(r)\dagger}(k), a^{(s)}(q)\} = 0.
\end{aligned}$$

The operators  $a, a^\dagger$  refer to particles, and  $b, b^\dagger$  to antiparticles, and  $\vec{k}^2 + m^2 = \epsilon^2$ . The text suppresses the spin indices  $r, s$  for simplicity.

<sup>§</sup>In the integration, we let

$$\int e^{-(k+p)^2} d^3k \rightarrow 4\pi e^{-p^2} \int e^{-k^2} k^2 dk$$

as a good approximation. Putting  $\vec{q}_i = \vec{p}_i = 0$  in the spinors allows us to integrate over the momentum wave functions directly.

<sup>||</sup>The integration is easily done in the limit  $m_\nu \rightarrow 0$ . Since for capture at rest,

$$|\vec{p}_\nu| = |\vec{p}_3 + \vec{q}_3| = (\vec{p}_3^2 + \vec{q}_3^2 + 2|\vec{p}_3||\vec{q}_3| \cos \theta)^{1/2} = \epsilon_\nu.$$

The integration over the energy  $\delta$  function is simply accomplished through the transformation.

<sup>11</sup>H. Primakoff, *Phys. Rev.* **31**, 802 (1959).

<sup>12</sup>J. P. Deutsche, L. Grenacs, P. Igo-Kemenes, P. Lipnik, and P. C. Macq, *Phys. Letters* **26B**, 315 (1968).

## Yield Curves for $\text{Li} + \text{Li}$ and $\text{Li} + \text{Be}$ Nuclear Reactions\*

H. W. Wyborny and R. R. Carlson

*Department of Physics and Astronomy, The University of Iowa, Iowa City, Iowa 52240*

(Received 17 December 1970)

Differential cross sections for  $\text{Li}^{6,7} + \text{Li}^{6,7}$  and  $\text{Li}^{6,7} + \text{Be}^9$  nuclear reactions leading to low-lying residual-nucleus states have been measured over the energy range from 4–14 MeV. In the  $\text{Li}^7(\text{Li}^7, \alpha)\text{Be}^{10}(3.37)$  case, the energy range was extended to 2.1 and 21 MeV. Striking enhancement and weakening of cross sections for formation of the 0.72-MeV state in  $\text{B}^{10}$  can be attributed to cluster structure of lithium nuclei. Resonance-like peaks are observed in some yields. Their general character is consistent with an extended-structure interpretation of the reaction mechanism.

### I. INTRODUCTION

Lithium-induced nuclear reactions could yield useful information about nuclear structure if the reaction mechanisms were well understood.<sup>1</sup> Unfortunately, this is not the case. At energies well below and well above the Coulomb barrier these reactions have been interpreted as primarily direct reactions.<sup>2,3</sup> Near the barrier the situation

is unclear. An example of this is afforded by the results of Synder and Waggoner for the  $\text{Li}^7 + \text{Be}^9$  reaction near 6 MeV.<sup>4</sup> Integrated cross sections for nearly all reaction channels studied showed a close proportionality to  $2J + 1$ , where  $J$  is the spin of a particular residual state; this is in agreement with a compound-nucleus mechanism.<sup>5</sup> However, cross sections were obtained from angular distributions which showed strong asym-

metrics about  $90^\circ$ .

Yield curves at  $0^\circ$  for lithium-induced reactions have shown large "resonance-like" peaks. Determinations of the relative contributions of compound-nucleus and direct-reaction mechanisms from such yield curves were attempted by Dzubay,<sup>6</sup> Seale,<sup>7</sup> and Aldrich.<sup>8</sup> Fluctuation analyses<sup>9</sup> were performed on yield curves for the  $C^{12}(Li^6, \alpha)N^{14}$ ,  $B^{10}(Li^6, \alpha)C^{12}$ , and  $Li^6(Li^6, \alpha)Be^8$  reactions, respectively. Dzubay concluded that the statistical compound-nucleus reaction mechanism provided a major contribution to his reaction, but the statistical sample was not large enough to preclude a direct-reaction contribution of up to 60%. Similar statements were made by Seale, Aldrich, Green,<sup>10</sup> and Johnson and Waggoner.<sup>11</sup> As these authors have indicated, their data sets only loosely met the criterion set forth by Ericson<sup>9</sup> as to whether a fluctuation analysis could be meaningfully applied. Ericson fluctuations are predicted to have their largest amplitude at 0 and  $180^\circ$ . However, some of the broad resonance-like peaks which have been observed in the  $Li^6 + B^{10}$ ,  $Li^6 + Li^6$ , and  $Li^7 + Li^7$   $0^\circ$  yield curves<sup>7,8,12</sup> occur in a somewhat regular pattern. This would indicate that they probably are not due to Ericson fluctuations.

Carlson and Johnson<sup>13</sup> have suggested a reaction mechanism which might explain such resonance-like structure in  $0^\circ$  yield curves. They have interpreted resonances in an  $\alpha$ -particle yield curve from the  $Li^7 + C^{12}$  reaction on the basis of an extended cluster structure of the lithium nucleus which becomes important when the projectile nucleus is making a "grazing collision" with the target nucleus. The partition energies of  $Li^6$  and  $Li^7$  into  $\alpha$ -deuteron and  $\alpha$ -triton clusters, respectively, are only 1.47 and 2.47 MeV. Partition energies for other cluster combinations are considerably higher. Resonance-like structure in  $0^\circ$  yield curves for lithium-induced reactions would, therefore, be expected to occur in those reactions where the  $\alpha$ -deuteron or  $\alpha$ -triton clusters could resonate with the target.

In order to test these ideas about the reaction mechanism in lithium-induced nuclear reactions, yield curves were measured for lithium and beryllium targets for as many residual states as was practical. Although a few yield curves were measured at 40 and  $175^\circ$ , the measurements reported here were taken at  $0^\circ$  from 4 to 14 MeV. Full details can be obtained from the unpublished work of Wyborný.<sup>14</sup> The  $Li^7(Li^7, \alpha)Be^{10}(3.36)$  yield curve was extended to an energy range from 2.1 to 21 MeV. A large collection of data was obtained to look for over-all patterns by making comparisons among various yield curves in regard to reaction model predictions. No detailed fits to the

data were sought.

## II. APPARATUS AND METHOD

Lithium ions were accelerated by the University of Iowa HVEC Van de Graaff positive-ion accelerator. Originating from a hot-filament source, the lithium beam could be accelerated to ground potential from a maximum of 6.5 MV. Hence, single-charged ions could attain energies of 6.5 MeV. Still higher energies (up to 14 MeV) were obtained by inserting an electron-stripping foil in the path of the beam at a point located 41.6% along the accelerator tube. Except for a special arrangement used in measuring one yield curve above 14 MeV, all of the data presented here were taken with a commercial 17-in. ORTEC Model 600 scattering chamber.

The lithium and beryllium targets ranged from 50–100 keV in thickness to the incident lithium beams. Beryllium targets were obtained by vacuum-evaporating beryllium granules from a tungsten dimple boat onto 0.0001-in. nickel foils. For bombarding energies  $\approx 7$  MeV, LiF was a suitable target material. For higher energies, the reactions from lithium on fluorine offered strong competition. No completely satisfactory lithium compound was found for running at the higher energies.  $Li_3Sb$ , formed by carefully heating stoichiometric amounts of Li and Sb under vacuum, was found to be the best compromise. It did react somewhat with atmospheric gases to form carbon and oxygen compounds; but carbon and oxygen nuclear reactions usually prevented analysis of only selective groups. In all cases 99.9% isotopically pure  $Li^6$  and  $Li^7$  metals and compounds were used.

Nickel foils ranging in thickness from 0.0002–0.0008 in. were used to stop the beam. They were attached directly behind the target, but physically separated to prevent excessive heating of the target material. Additional foil (up to 0.0018 in.) had to be inserted directly in front of the detectors when using the  $Li^{+++}$  beam. This additional foil was necessary to stop a small contaminant beam of deuterons ( $\sim 10^{-8}$   $\mu A$ ) which had the same charge/momentum ratio as triply charged lithium. (The source of deuterons could have been either a minute leak in a deuterium source bottle or just residual deuterium gas which was left in the accelerating tube from previous usage.)

Accurate measurement of the number of beam particles striking the target was essential in measuring the yield curves. This was accomplished with an enclosed aluminum cylinder which surrounded the target. Holes for target insertion, beam entry, and reaction-product exit comprised approximately 0.3% of the total solid angle as

viewed from the center of the target. Assuming a somewhat isotropic emission of secondary electrons, charge collection from this trap (plus the target rod) should have been a measure of the beam current striking the target, to better than 1%.

A second purpose was also accomplished with the aluminum cylinder. The insulated copper rod which supported the cylinder extended to the outside of the chamber and was partly submerged in liquid nitrogen. When cold, the walls of the aluminum enclosure served as an effective pump for both oxygen and hydrocarbon molecules. Upon cooling, the base vacuum in the chamber improved from roughly  $1.5 \times 10^{-6}$  Torr to  $5 \times 10^{-7}$  Torr. This "freezing out" of hydrocarbon contaminants reduced carbon buildup on the targets to a negligible quantity.

A telescoped  $\Delta E$ ,  $E$  detector system was used to provide particle identification. The  $\Delta E$  detector was a 40- $\mu$  totally depleted silicon surface-barrier detector. The  $E$  detector was lithium drifted and had a 3-mm depletion depth. Both had 50-mm<sup>2</sup> surface areas and their aperture subtended a full angle of  $3.3^\circ$  at the beam spot. Pulses from the detectors were amplified and pulse-height-analyzed with conventional electronics.

Results of the pulse-height analysis were accumulated in an on-line computer which was later used to separate particle types and groups, and to sum the number of counts in the various groups.<sup>11</sup> The final reduction of the data into a meaningful form was done with a program on the University of Iowa Computer Center's IBM Model 360 digital computer. The program normalized between energies by comparing the current integrator input at a particular energy to the average integrator input of all energies for that particular beam-target combination. A normalization factor for obtaining absolute values was also included, and an average over energy was calculated.

Recently published cross sections for  $\text{Li}^7 + \text{Be}^9$  angular distributions by Snyder and Waggoner<sup>4</sup> were used as the basis for determining absolute numbers for the  $\text{Li}^7 + \text{Be}^9$  reaction channels.  $\text{Li}^6 + \text{Be}^9$  cross sections were obtained by using a  $\text{Li}^7$  beam, followed by a  $\text{Li}^6$  beam on the same Be target at the same energy. The  $\text{Li}^7$  beam run provided a measure of the target thickness and geometrical factors.

Absolute differential cross sections have been reported by Carlson and Wyborny<sup>15</sup> for angular distributions of reaction products from the  $\text{Li}^7 + \text{Li}^7$  reaction. The absolute values were obtained from measured yields of a target infinitely thick to the lithium beam together with relative yields

of a thin target measured as a function of energy, and the energy-loss rates of  $\text{Li}^7$  ions, also as a function of energy.<sup>16</sup> These corrected absolute values were used to normalize the present results for the  $\text{Li}^7 + \text{Li}^7$  reaction channels. Knowing the  $\text{Li}^7 + \text{Li}^7$  cross sections,  $\text{Li}^6$  (beam) +  $\text{Li}^7$  (target) absolute values were determined in the same manner as the  $\text{Li}^6 + \text{Be}^9$  cross sections were determined. Here  $\text{Li}^7$  and  $\text{Li}^6$  beams were run in sequence on the same  $\text{Li}^7$  target. For  $\text{Li}^7$  (beam) +  $\text{Li}^6$  (target), a carefully weighed mixture of  $\text{Li}^6\text{F}$  and  $\text{Li}^7\text{F}$ , containing an equal number of  $\text{Li}^6$  and  $\text{Li}^7$  atoms, was evaporated to make a "50-50" target. Here a single run with a  $\text{Li}^7$  beam provided  $\text{Li}^7$  (beam) +  $\text{Li}^6$  (target) data that could be normalized directly to  $\text{Li}^7 + \text{Li}^7$  cross sections. Several peaks in the superimposed pulse-height spectra from the isotopically distinct targets were separated kinematically. With this same "50-50" target a  $\text{Li}^6$  beam provided normalization of  $\text{Li}^6 + \text{Li}^6$  data to the  $\text{Li}^6$  (beam) +  $\text{Li}^7$  (target) cross sections.

The statistical error of each data point is taken to be the standard deviation. The error bars on the data points to be presented are a reflection of this error only. Neglecting statistical error of individual data points, error in absolute cross section for the reactions is expected to be less than 15%.

### III. ARGONNE NATIONAL LABORATORY ARRANGEMENT

The Argonne National Laboratory FN tandem Van de Graaff was used to extend the  $\text{Li}^7(\text{Li}^7, \alpha)\text{-Be}^{10}(3.37)$  yield curve to energies above 14 MeV. A much less sophisticated chamber was employed for these measurements.<sup>7</sup> Essentially, it was a Faraday cup with the target located inside the cup and the detector behind the cup at  $0^\circ$  to the beam. A negative 300-V potential on the beam pipe in front of the cup served to inhibit backstreaming of electrons knocked from the target by the incident beam. The target, its backing (the stopping foil), and the Faraday cup were all in physical and electrical contact for the purpose of charge collection. A lithium oxide (some hydroxide) target was formed by evaporating lithium metal onto a thin nickel backing and then admitting pure oxygen into the evaporation chamber.

A 1000- $\mu$  solid-state detector was used to detect the  $\alpha$  particles. The detector subtended a full angle of  $8.3^\circ$  at the beam spot. No identification of particle type was necessary here, because the particles of interest arrived at the detector with energy well-resolved from other groups. After collecting the data for a particular energy, the memory content of the pulse-height analyzer

TABLE I. Energy-averaged laboratory differential cross sections in mb/sr for the Li + Li reactions. Only data above Coulomb barriers were included in the averages.  $r_0$  was taken to be 1.44 in calculating the radii from  $r = r_0 A^{1/3}$ .

Reaction	Ground-state										
	Q value (MeV)	$E^*$ (MeV)	$\frac{d\sigma}{d\Omega}$								
$\text{Li}^6(\text{Li}^6, p)\text{B}^{11}$	12.220	0.00	0.31	2.12	0.15	4.44	0.34	5.02	0.15	6.74 6.79	0.86
$\text{Li}^6(\text{Li}^6, d)\text{B}^{10}$	2.989	0.00	1.65	0.72	12.1	1.74	0.04	2.15	1.96		
$\text{Li}^6(\text{Li}^6, t)\text{B}^9$	0.808	0.00	1.40								
$\text{Li}^6(\text{Li}^6, \alpha)\text{Be}^8$	20.808	0.00	0.5								
$\text{Li}^7(\text{Li}^6, p)\text{B}^{12}$	8.336	0.00	0.52	0.95	0.33	1.67	0.40	2.62 2.72	0.42		
$\text{Li}^7(\text{Li}^6, d)\text{B}^{11}$	7.192	0.00	2.43	2.12	1.23	4.44	2.30			5.02	4.14
$\text{Li}^7(\text{Li}^6, t)\text{B}^{10}$	1.994	0.00	2.46	0.72	2.52	1.74	0.19	2.15	4.69		
$\text{Li}^7(\text{Li}^6, \alpha)\text{Be}^9$	15.220	0.00	1.10								
$\text{Li}^6(\text{Li}^7, p)\text{B}^{12}$	8.336	0.00	0.24	0.95	0.22	1.67	0.21	2.62 2.72	0.45		
$\text{Li}^6(\text{Li}^7, d)\text{B}^{11}$	7.192	0.00	5.50	2.12	0.90	4.44	1.86			5.02	2.28
$\text{Li}^6(\text{Li}^7, t)\text{B}^{10}$	1.994	0.00	1.40	0.72	15.6						
$\text{Li}^6(\text{Li}^7, \alpha)\text{Be}^9$	15.220	0.00	1.69								
$\text{Li}^7(\text{Li}^7, p)\text{B}^{13}$	5.964	0.00	0.24	3.48 3.53	0.60	3.68 3.71	1.65	4.13	0.28	5.01	0.84
$\text{Li}^7(\text{Li}^7, d)\text{B}^{12}$	3.308	0.00	0.67								
$\text{Li}^7(\text{Li}^7, t)\text{B}^{11}$	6.197	0.00	2.60	2.12	1.46	4.44	4.07	5.02	4.40		
$\text{Li}^7(\text{Li}^7, \alpha)\text{Be}^{10}$	14.783	0.00	0.18	3.37	2.08						

was punched onto IBM computer cards, and the University of Iowa IBM 360 computer was used for final reduction of data.

#### IV. RESULTS

A wide diversity in shapes and in magnitudes of cross sections was seen in the large number of yield curves which were measured. In general, cross sections of Li + Li reaction products were nearly an order-of-magnitude larger than those of Li + Be. The energy averages of the  $0^\circ$  cross sec-

tions above the Coulomb barrier are given in Table I for Li + Li and in Table II for Li + Be. The averages were usually over the energy range from the Coulomb barrier to 14 MeV although reaction groups from contaminants interfered in some energy ranges. Also, proton groups for high-Q reactions could not be stopped for high bombarding energies

The 0.72-MeV state of  $\text{B}^{10}$  is seen to be very strongly populated by both the  $\text{Li}^6(\text{Li}^6, d)\text{B}^{10}$  and  $\text{Li}^6(\text{Li}^7, t)\text{B}^{10}$  reactions but not particularly enhanced by the  $\text{Li}^7(\text{Li}^6, t)\text{B}^{10}$  reaction. The enhance-

TABLE II. Energy-averaged laboratory differential cross sections in  $\mu\text{b}/\text{sr}$  for the Li + Be reactions. Only data above Coulomb barriers were included in the averages.  $r_0$  was taken to be 1.44 in calculating the radii from  $r = r_0 A^{1/3}$ .

Reaction	Ground state										
	Q value (MeV)	$E^*$ (MeV)	$\frac{d\sigma}{d\Omega}$								
$\text{Be}^9(\text{Li}^6, p)\text{C}^{14}$	15.130	0.00	4.5	6.10	19						
$\text{Be}^9(\text{Li}^6, d)\text{C}^{13}$	9.178	0.00	90	3.09	230	3.68 3.85	510				
$\text{Be}^9(\text{Li}^6, t)\text{C}^{12}$	10.489	0.00	60	4.44	410			7.65	115		
$\text{Be}^9(\text{Li}^6, \alpha)\text{B}^{11}$	14.346	0.00	230	2.12	200						
$\text{Be}^9(\text{Li}^7, p)\text{C}^{15}$	9.096	0.00	28	0.75	78						
$\text{Be}^9(\text{Li}^7, d)\text{C}^{14}$	10.102	0.00	107	6.10	150						
$\text{Be}^9(\text{Li}^7, t)\text{C}^{13}$	8.183	0.00	210	3.09	190	3.68 3.85	1190				
$\text{Be}^9(\text{Li}^7, \alpha)\text{B}^{12}$	10.463	0.00	500	0.95	700			1.67	640	2.62 2.72	580

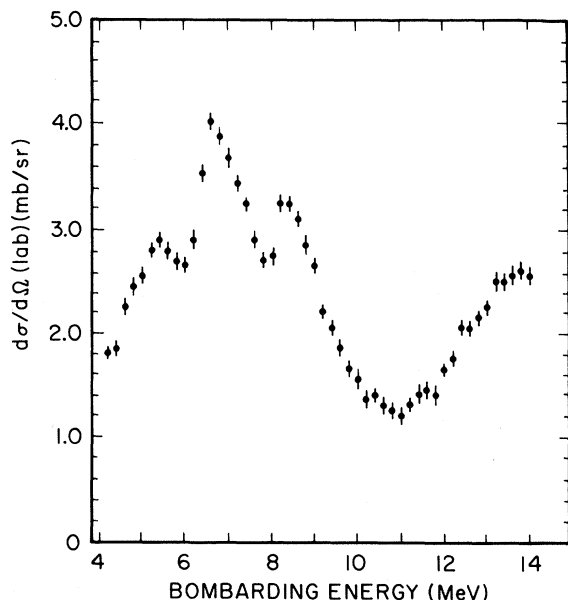


FIG. 1. Yield curve for  $\text{Li}^7(\text{Li}^6, d)\text{B}^{11}(0.00)$  at  $0^\circ$ . Statistical error only shown on points.

ment of this state by the first two reactions may be attributed to the transfer of an  $l = 0$   $\alpha$  particle from the projectile to the target nucleus. This is in agreement with the  $\alpha$ - $d$  and  $\alpha$ - $t$  cluster pictures of  $\text{Li}^6$  and  $\text{Li}^7$ , respectively.

The 1.74-MeV state of  $\text{B}^{10}$  is seen to be very weakly populated by both the  $\text{Li}^6(\text{Li}^6, d)\text{B}^{10}$  and  $\text{Li}^7(\text{Li}^6, t)\text{B}^{10}$  reactions. This state has spin  $0^+$

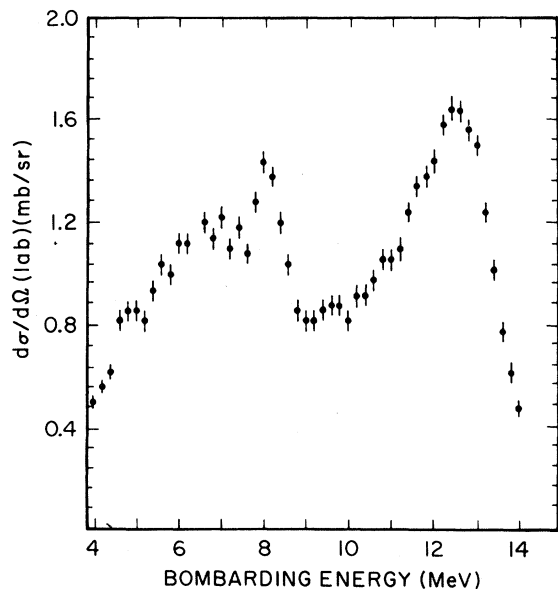


FIG. 2. Yield curve for  $\text{Li}^7(\text{Li}^6, \alpha)\text{Be}^9(0.00)$  at  $0^\circ$ . Statistical error only shown on points.

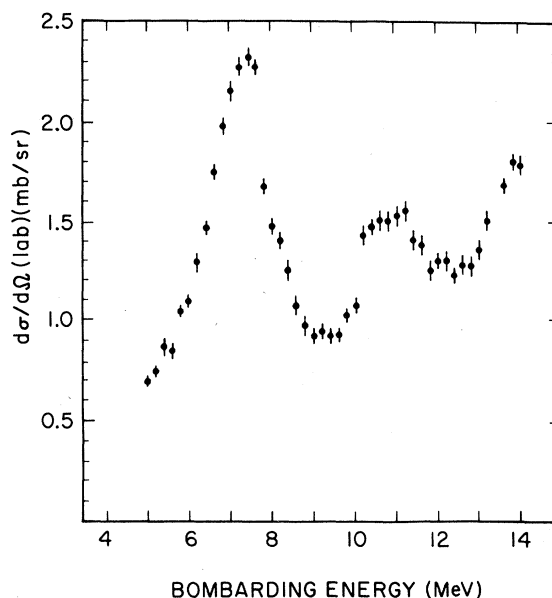


FIG. 3. Yield curve for  $\text{Li}^6(\text{Li}^7, t)\text{B}^{10}(0.00)$  at  $0^\circ$ . Statistical error only shown on points.

and  $T = 1$ . The weak population has been interpreted as resulting from the inability to form the  $0^+$   $\text{B}^{10}$  state by adding an  $\alpha$  cluster from a lithium nucleus to a  $1^+$   $\text{Li}^6$  nucleus.<sup>17</sup> The generally low values for proton reactions is also in accord with the cluster picture of the lithium nuclei. The low value of the cross section for  $\text{Li}^7(\text{Li}^7, \alpha)\text{Be}^{10}(0.00)$  is not understood.

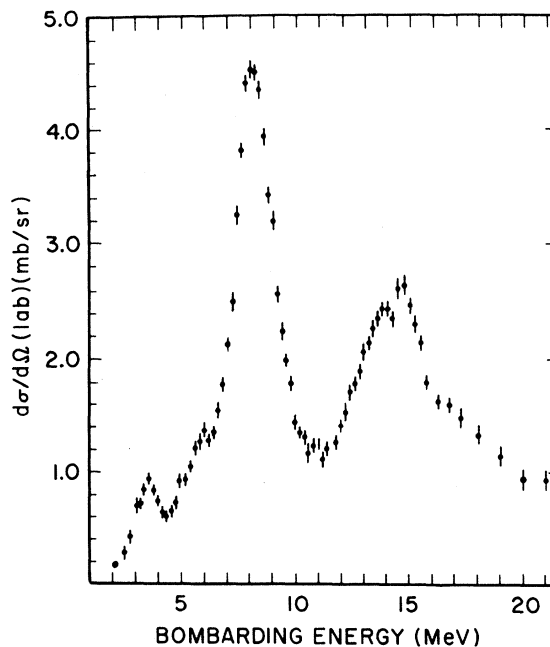


FIG. 4. Yield curve for  $\text{Li}^7(\text{Li}^7, \alpha)\text{Be}^{10}(3.37)$  at  $0^\circ$ . Statistical error only shown on points.

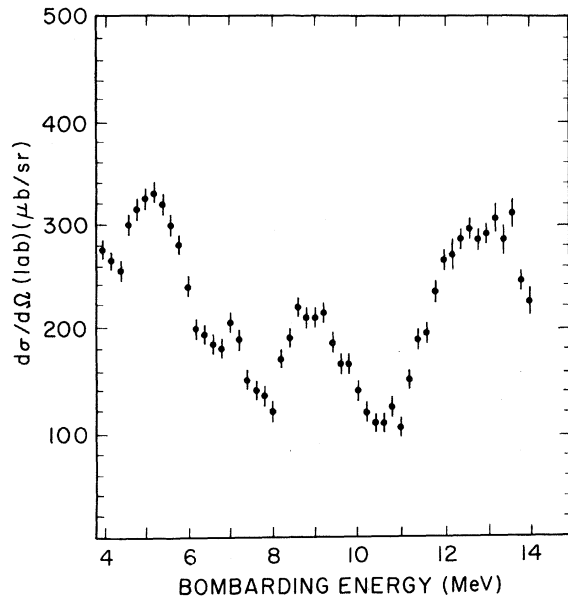


FIG. 5. Yield curve for  $\text{Be}^9(\text{Li}^7, t)\text{C}^{13}(0.00)$  at  $0^\circ$ . Statistical error only shown on points.

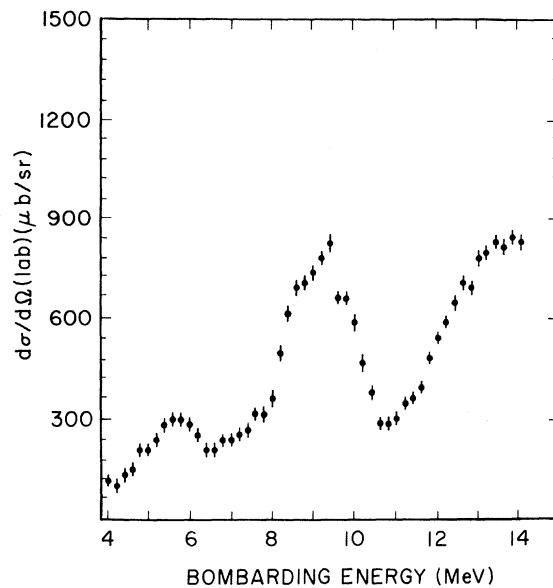


FIG. 6. Yield curve for  $\text{Be}^9(\text{Li}^7, \alpha)\text{B}^{12}(0.00)$  at  $0^\circ$ . Statistical error only shown on points.

Probably the most distinctive feature observed in the yield curves was a characteristic type of peaking in selective reaction channels. These particular reactions have yield curves which have broad peaks ( $\sim 1\text{--}4$  MeV full width at half maximum) and pronounced peak-to-valley ratios ( $> 2/1$ ).

Outstanding examples are shown in Figs. 1–4 for Li + Li reactions, and Figs. 5 and 6 for Li + Be reactions.

Results shown in Fig. 4 were extended to higher-bombarding energies than the other results by use of the Argonne National Laboratory FN tandem

TABLE III. Reactions with  $0^\circ$  yield curves containing resonant-type peaks.

Reaction	Approximate peak frequency in 4–14-MeV interval	Location of yield curve
$\text{Li}^6(\text{Li}^6, \alpha_0)\text{Be}^8(0.00)$	2	Ref. 1
$\text{Li}^7(\text{Li}^6, d_0)\text{B}^{11}(0.00)$	$1\frac{1}{2}$	Fig. 1
$\text{Li}^7(\text{Li}^6, \alpha_0)\text{Be}^9(0.00)$	2	Fig. 2
$\text{Li}^6(\text{Li}^7, t_0)\text{B}^{10}(0.00)$	$2\frac{1}{2}$	Fig. 3
$\text{Li}^7(\text{Li}^7, \alpha_0)\text{Be}^{10}(0.00)$	$1\frac{1}{2}$	Ref. 14
$\text{Li}^7(\text{Li}^7, \alpha_1)\text{Be}^{10}(3.37)$	$1\frac{1}{2}$	Fig. 4
$\text{Be}^9(\text{Li}^7, t_0)\text{C}^{13}(0.00)$	3	Fig. 5
$\text{Be}^9(\text{Li}^7, \alpha_0)\text{B}^{12}(0.00)$	$2\frac{1}{2}$	Fig. 6
$\text{Be}^9(\text{Li}^7, \alpha_1)\text{B}^{12}(0.95)$	$3\frac{1}{2}$	Ref. 14
$\text{Be}^9(\text{Li}^7, \alpha_2)\text{B}^{12}(1.67)$	3 or 4	Ref. 14
$\text{B}^{10}(\text{Li}^6, \alpha_0)\text{C}^{12}(0.00)$	3	Ref. 7
$\text{C}^{12}(\text{Li}^6, d_0)\text{O}^{16}(0.00)$	4 or 5	Ref. 11
$\text{C}^{12}(\text{Li}^6, \alpha_0)\text{N}^{14}(0.00)$	4	Ref. 11
$\text{C}^{12}(\text{Li}^7, \alpha_0)\text{N}^{15}(0.00)$	4	Ref. 13
$\text{O}^{16}(\text{Li}^6, \alpha_n)\text{F}^{18}(0.00)$	6	Ref. 16

Van de Graaff. Data from 2.1–14 MeV were taken at the University of Iowa and data from 12–21 MeV, at Argonne National Laboratory.

Table III gives a list of the reactions whose  $0^\circ$  yield curves contain broad peaks. In addition to the data shown here, other reactions are listed where such peaks have been observed. It is significant that such curves are observed only for  $(\text{Li}^6, d)$ ,  $(\text{Li}^6, \alpha)$ ,  $(\text{Li}^7, t)$ , and  $(\text{Li}^7, \alpha)$  reactions. Such an observation suggests that cluster-transfer reactions play an important role at forward angles in lithium reactions – at least in some selective channels.

The high excitation of the compound nucleus in these reactions (from 23–33 MeV) would argue against any of the observed peaks being due to states of the compound nucleus. The breadth and

regularity of the peaks also argue against an interpretation in terms of Ericson fluctuations although such an interpretation cannot be disproved. On the other hand, the cross section varies more than one would expect for a direct-reaction mechanism.

An alternative to these two extremes has been suggested by Carlson and Johnson<sup>13</sup> for lithium-induced reactions. Because of the cluster structure of lithium nuclei, it is suggested that these nuclei form extended structures when near other nuclei and that resonances occur. These resonances can enhance the forward yield of reactions at the appropriate energies. The heavier the other nucleus, the more closely spaced these resonances become. Table III shows that there is a trend in this direction.

---

\*Work supported in part by the National Science Foundation.

<sup>1</sup>R. R. Carlson, in *Nuclear Research with Low-Energy Accelerators*, edited by J. B. Marion and D. M. Van Patter (Academic Press Inc., New York, 1967), p. 475.

<sup>2</sup>G. C. Morrison, *Phys. Rev.* **121**, 182 (1961).

<sup>3</sup>K. Bethge, K. Meier-Ewert, K. Pfeiffer, and R. Bock, *Phys. Rev. Letters* **24B**, 663 (1967).

<sup>4</sup>F. D. Snyder and M. A. Waggoner, *Phys. Rev.* **186**, 999 (1969).

<sup>5</sup>N. MacDonald, *Nucl. Phys.* **33**, 110 (1962).

<sup>6</sup>T. G. Dzubay, *Phys. Rev.* **158**, 977 (1967).

<sup>7</sup>W. A. Seale, *Phys. Rev.* **160**, 809 (1967).

<sup>8</sup>B. D. Aldrich, M.S. thesis, University of Iowa (unpublished).

<sup>9</sup>T. Ericson, *Ann. Phys. (N.Y.)* **23**, 390 (1963).

<sup>10</sup>M. W. Greene, *Phys. Rev.* **176**, 1204 (1968).

<sup>11</sup>D. J. Johnson and M. A. Waggoner, *Phys. Rev. C* **2**, 41 (1970).

<sup>12</sup>H. W. Wyborny, M.S. thesis, University of Iowa (unpublished).

<sup>13</sup>R. R. Carlson and D. J. Johnson, *Phys. Rev. Letters* **25**, 172 (1970).

<sup>14</sup>H. W. Wyborny, Ph.D. thesis, University of Iowa (unpublished).

<sup>15</sup>R. R. Carlson and H. W. Wyborny, *Phys. Rev.* **178**, 1529 (1969).

<sup>16</sup>Earlier published cross sections were based on older energy-loss tables which gave 5% higher values for the cross section than the values given here.

<sup>17</sup>G. C. Morrison, *Phys. Rev. Letters* **5**, 565 (1960).